Journal of Molecular Neuroscience
https://doi.org/10.1007/s12031-017-1023-9

Basic Fibroblast Growth Factor Protects Astrocytes Against Ischemia/Reperfusion Injury by Upregulating the Caveolin-1/VEGF Signaling Pathway

Meixia Liu[1] · Yudan Wu[1] · Yidian Liu[1] · Zhenzhen Chen[1] · Shujuan He[1] · Huimei Zhang[1] · Liang Wu[1] · Fengxia Tu[1] · Yun Zhao[1] · Chan Liu[1] · Xiang Chen[1]

Received: 14 October 2017 / Accepted: 20 December 2017

Abstract
A previous in vivo study demonstrated that intracerebroventricular injection of basic fibroblast growth factor (bFGF) in middle cerebral artery occlusion rats increased the expression of caveolin-1 (cav-1) and vascular endothelial growth factor (VEGF) in cerebral ischemia penumbra. Because astrocytes are the largest population in the brain, the aim of this in vitro study was to investigate the influence of bFGF on cav-1 and VEGF expression in rat astrocytes following oxygen glucose deprivation/reoxygenation (OGD/R). For this, an ischemic model in vitro of oxygen glucose deprivation lasting for 6 h, followed by 24 h of reoxygenation was used. Primary astrocytes from newborn rats were pre-treated with siRNA targeting bFGF before OGD/R. Cell viability was measured by a CCK-8 assay. The protein and mRNA expressions of bFGF, cav-1, and VEGF were evaluated by western blotting, immunofluorescence staining, and reverse transcription-quantitative polymerase chain reaction. The results showed that OGD/R reduced cell viability, which was decreased further following bFGF knockdown; however, restoring bFGF improved cell survival. A cav-1 inhibitor abrogated the effect of bFGF on cell viability. The expression levels of bFGF mRNA, bFGF protein, cav-1 mRNA, cav-1 protein, and VEGF protein were higher in OGD/R astrocytes. bFGF knockdown markedly decreased the expression levels of cav-1 mRNA, cav-1 protein, and VEGF protein, which were effectively reversed by exogenous bFGF treatment. Moreover, exogenous bFGF treatment significantly increased the expression levels of cav-1 mRNA, cav-1 protein, and VEGF protein in OGD/R astrocytes; however, a cav-1 inhibitor abolished the effect of bFGF on VEGF protein expression. These results suggested that bFGF may protect astrocytes against ischemia/reperfusion injury by upregulating caveolin-1/VEGF signaling pathway.

Keywords Basic fibroblast growth factor · Caveolin-1 · Vascular endothelial growth factor · OGD/R · Primary astrocytes

Introduction

Stroke is the most common cause of death in China and the major cause of morbidity and mortality worldwide. Because only a small group of stroke patients benefit from thrombolytic therapy, recent investigations into stroke have concentrated on regenerative therapies and neuroprotective treatment (Lee et al. 2011; Yamashita et al. 2006). Many studies have demonstrated that several endogenous growth factors such as basic fibroblast growth factor (bFGF) and brain-derived neurotrophic factor (BDNF) promote neurogenesis and rescue cell death after ischemic stroke (Bethel et al. 1997; Kalluri and Dempsey 2008). bFGF, mainly secreted from astrocytes in the adult brain, is an efficient mitogen that promotes the proliferation and differentiation of a wide range of neuron-ectodermal and mesodermal cell types (Basilico and Moscatelli 1992). Several studies have demonstrated that bFGF induces the neuronal differentiation of stem cells derived from various mesenchymal tissues, including endometrial (Noureddini et al. 2012), skeletal muscle (Kang et al. 2013), and adipose tissues (Jang et al. 2010). Studies have also shown that bFGF strongly facilitates the proliferation and differentiation of neural stem/progenitor cells (NSPCs) in the subventricular zone (SVZ) and circumventricular organs (CVOs) as well as several other new sites along the third and

✉ Xiang Chen
chenxiangnj2005@163.com

[1] Physical Medicine and Rehabilitation Center, The Second Affiliated Hospital & Yuying Children's Hospital of Wenzhou Medical University, No. 109, Xueyuanxi Road, Wenzhou, Zhejiang 325027, China

Published online: 03 January 2018

fourth ventricles after stroke (Lin et al. 2015), and that bFGF dominates NSPC differentiation into neurons instead of astrocytes (Li et al. 2012; Li et al. 2016). Moreover, under various injury conditions, bFGF improved the function of the blood-nerve barrier and blood-brain barrier (Proia et al. 2008; Shimizu et al. 2011). These reports indicate that bFGF plays an important role in neurogenesis and neuroprotection after stroke, which indicate it might be a potential drug for stroke treatment.

Caveolin-1 (cav-1), an iconic structural protein of caveolae, regulates cellular signal transduction, transcytosis, endocytosis, molecular transport, normal tissue growth, embryonic vessel development, and pathological processes (such as tumor growth, ischemia) (Liu et al. 2002; Mundy et al. 2002; Navarro et al. 2004). Vascular endothelial growth factor (VEGF) has a crucial role in angiogenesis (Hansen et al. 2008; Zhang and Chopp 2002). VEGF protected neurons from ischemic insults and promoted neurogenesis after cerebral ischemic injury (Ma et al. 2012; Pignataro et al. 2015). Our previous in vivo studies used a cav-1 inhibitor to demonstrate that treadmill training in a rat model of middle cerebral artery occlusion (MCAO) decreased cerebral infarct volume, promoted neurological recovery, and facilitated angiogenesis and neurogenesis through upregulating the caveolin-1/VEGF signaling pathway (Gao et al. 2014; Zhao et al. 2017). Other studies have also shown that cav-1 gene ablation in mice leads to increased cerebral infarction volume, increased cell death, decreased VEGF expression, and impaired angiogenesis (Chidlow and Sessa 2010; Jasmin et al. 2007). These studies indicate that the caveolin-1/VEGF signaling pathway plays a significant role in the functional recovery of cerebral ischemic stroke.

Based on the above, we previously showed that the in vivo intracerebroventricular injection of bFGF in MCAO rats increased cav-1 and VEGF expression in the ischemia penumbra of rat brain. A recent study has also demonstrated that bFGF improved the functional recovery in rats with spinal cord injury by increasing the expression of cav-1 and reducing the expression of matrix metalloproteinase-9 (Ye et al. 2016). Therefore, we hypothesized that bFGF functions as the upstream molecule of the caveolin-1/VEGF signaling pathway in stroke recovery. Astrocytes are major cells of the central nervous system (CNS) and play a vital role in regulating neural stem cell proliferation and differentiation (Li et al. 2014; Yang et al. 2014). In response to cerebral ischemia, astrocytes become activated and release various growth factors, including bFGF (Yang et al. 2014) and VEGF (Koyama et al. 2012; Lafuente et al. 2012), which are beneficial for stroke recovery. In addition, astrocytes universally express cav-1. The current study generated an in vitro model of oxygen glucose deprivation/reoxygenation (OGD/R) to mimic cerebral ischemia/reperfusion (I/R) injury in vivo, and then investigated whether bFGF closely affected cav-1 and VEGF expression in primary cultured astrocytes, by using bFGF knockdown, exogenous bFGF treatment and cav-1 inhibitor treatment. Our results showed that bFGF significantly increased cav-1 and VEGF expression in primary astrocytes under OGD/R conditions, and a cav-1 inhibitor abolished the effect of bFGF on VEGF expression. Furthermore, bFGF protected astrocytes against OGD/R-induced injury, and a cav-1 inhibitor abrogated the protective effect of bFGF. This indicates that bFGF may protect astrocytes from I/R injury by upregulating the caveolin-1/VEGF signaling pathway.

Materials and Methods

Extraction and Culture of Primary Astrocytes

All neonatal *Sprague-Dawley* rats (1–2 day old, male or female) in this study were obtained from the Animal Experiment Center of Wenzhou Medical University (Wenzhou, China). All animal procedures were approved by the Ethics Committee of Wenzhou Medical University (Wenzhou, China) and followed NIH guidelines. The number of rats used in this study and their pain during experiments was minimized.

Primary astrocyte cultures were extracted from the cerebral cortex of 10 neonatal *Sprague-Dawley* rats as described previously (Lv et al. 2015; McCarthy and de Vellis 1980). The cortex tissue was digested with 0.125% trypsin at 37 °C for 5 min, and the cultures were grown in high-glucose DMEM medium (Gibco, USA) containing 10% fetal bovine serum (Gibco, USA), 100 units/mL penicillin, and 100 mg/mL streptomycin in culture bottles previously coated with poly-L-lysine (0.1 mg/mL; Sigma) overnight. They were cultured in a 5% CO_2 incubator (Thermo Fisher Scientific, Inc.) at 37 °C, and the medium was changed every 3 days. When the cells reached 80% confluence at approximately 10–12 days, the mixed cultures were shaken at 37 °C, 200 rpm for 18 h to remove oligodendroglia and microglia. The purified astrocytes were then trypsinized and subcultured. Astrocytes were identified by their typical morphology and positive staining for glial fibrillary acidic protein (GFAP), a specific marker of astrocytes. Results showed that cells had a paving stone morphology after 10–12 days of primary culture and more than 95% of the cultured cells were astrocytes as identified by immunofluorescent staining for GFAP (data was not shown).

Groups and Cell Treatment

Astrocytes were randomly divided into nine groups: (1) control group, astrocytes without treatment; (2) NC siRNA group, astrocytes transfected with negative lentivirus for 72 h, (LVCON053): 5′-TTCTCCGAACGTGTCACGT-3′; (3) sibFGF group, astrocytes transfected with a lentivirus carrying siRNA targeting bFGF for 72 h, LV-Fgf2-RNAi: 5′-TCAA

GGGAGTGTGTGCGAA-3′; (4) OGD/R group, astrocytes subjected to OGD/R; (5) NC siRNA + OGD/R group, astrocytes subjected to OGD/R after 72 h of transfection with LVCON053; (6) sibFGF + OGD/R group, astrocytes subjected to OGD/R after 72 h of transfection with LV-Fgf2-RNAi; (7) OGD/R + bFGF group, astrocytes subjected to OGD/R after 72 h of treatment with 20 ng/ml bFGF; (8) NC siRNA + OGD/R + bFGF group, astrocytes subjected to OGD/R after 72 h of transfection with LVCON053 and treatment with 20 ng/ml bFGF; and (9) sibFGF + OGD/R + bFGF group, astrocytes subjected to OGD/R after 72 h of transfection with LV-Fgf2-RNAi and treatment with 20 ng/ml bFGF (recombinant rat FGF-basic, 400-29, PeproTech, USA).

To further study, astrocytes were divided into another two groups: (1) OGD/R + bFGF group, as mentioned above and (2) OGD/R + bFGF + cav-1 inhibitor group, astrocytes subjected to OGD/R after 72 h of treatment with 20 ng/ml bFGF and 100 μmol/L daidzein (S1849, Selleckchem, USA).

Construction of sibFGF Lentivirus and Cell Transfection

The construction of the lentiviruses was performed by Shanghai Genechem Co. Ltd. (Shanghai, China). The lentiviral vector number is GV115, the element order is hU6-MCS-CMV-EGFP, and the cloning sites are *Age*I and *Eco*RI. Because the lentiviruses stably express green fluorescent protein (GFP), the optimal multiplicity of infection (MOI) and infection duration were determined according to the expression level of GFP under fluorescence microscopy (Olympus, Japan) using different concentration gradients of lentivirus. The MOI was calculated as follows: MOI = (viral titer × virus volume) / cell number. Briefly, the cells were inoculated in six-well plates at a concentration of 5×10^4 cells/ml with corresponding media. Then, 24 h after cultivation, they were transfected with either LV-Fgf2-RNAi or LVCON053 for 12 h at a MOI of 20. LVCON053 served as the negative control. The medium was then changed with corresponding media. At 72 h following lentivirus transfection, the transfection efficiency was observed under a fluorescence microscope, and the efficiency of bFGF knockdown was determined by reverse transcription-quantitative polymerase chain reaction (RT-qPCR).

Establishment of OGD/R Model

After lentivirus transfection, cells were washed two times with phosphate-buffered saline (PBS) and cultured in glucose-free DMEM medium (Gibco) in a hypoxic chamber (Thermo Fisher Scientific, Inc.) containing 94% N_2, 5% CO_2, and 1% O_2 at 37 °C for 6 h. After OGD, the glucose-free DMEM medium was changed with normal medium and the cells were immediately transferred into a 5% CO_2 incubator for 24 h of recovery at 37 °C. The cells in the first three groups were not treated with OGD.

Cell Viability Assay

The number of surviving astrocytes following OGD/R and/or lentivirus transfection was determined by a CCK-8 assay. Astrocytes were plated in 96-well plates (3×10^4 cells/ml in 100 μL medium) with corresponding media. After lentivirus transfection and OGD/R treatment, 10 μL of CCK-8 solution (DOJINDO, Japan) was added to each well, and the cells were then incubated for another 30 min at 37 °C. Optical density (OD) values were measured at a wavelength of 450 nm using a multimode reader (ECX 800, BIO-TEK, USA). A linear relationship between the OD values and viable cell density was obtained. The assay was repeated at least three times and each assay was performed in triplicate. The calculation formula of cell survival rate was below: cell survival rate = (OD experiment − OD blank) / (OD control − OD blank) × 100%.

RNA Extraction and RT-qPCR

RT-qPCR was performed to examine the mRNA expression levels of bFGF and cav-1. Total RNA was extracted from astrocytes with TRIzol Reagents (Invitrogen) according to the manufacturer's protocol and was subsequently reverse-transcribed into cDNA using a RevertAid First Strand cDNA Synthesis kit (Thermo Fisher Scientific, Inc.) at 42 °C for 1 h, 25 °C for 5 min, and 70 °C for 5 min. The products of reverse transcription were used for real-time qPCR. The primer information is listed in Table 1. LightCycler 480 SYBR Green I Master (Roche, USA) was used for PCR reactions. The setting of the thermocycling program was as follows: initial denaturation at 95 °C for 5 min; 45 cycles of denaturation at 95 °C for 10 s, annealing at 60 °C for 10 s and extension at 72 °C for 10 s; and a final extension at 40 °C for 30 s. The data of quantification cycle (Cq) was collected by LightCycler®480 Software release 1.5.0 SP4 (Roche, USA). All samples were read in triplicate, and the values were normalized to Tubulin 3 expression. The $2^{-\Delta\Delta Cq}$ method was used to analyze the relative quantification of mRNA expression. The calculation formula for fold change in target gene cDNA relative to reference gene cDNA was as follows: fold change $= 2^{-\Delta\Delta Cq}$, $\Delta\Delta Cq = (Cq_{Sample} - Cq_{Tubulin\ 3}) - (Cq_{Control} - Cq_{Tubulin\ 3})$.

Cell Proteins Extraction and Western Blotting

Lysis in RIPA buffer was used to extract proteins from primary astrocytes (Beyotime Biotechnology, China). An Enhanced BCA Protein Assay kit (Beyotime Biotechnology, China) was used to determine the protein concentration of samples. Equal amounts of protein extracts (30 μg) were separated by

Table 1 Primer sequences used for real-time qPCR

Gene	Gene ID	Primer sequence (5′–3′)	Product length (bp)
bFGF	NC_005101.4	F: TCCATCAAGGGAGTGTGTGC R: TCCGTGACCGGTAAGTGTTG	139
cav-1	NM_031556.3	F: ATCTGGGCAGTTGTACCGTG R: CGTGCTGATGCGGATATTGC	144
Tubulin 3	NM_139254.2	F: CCGCCTGCCTCTTCGTCT R: GGTCTATGCCATGCTCGTCAC	131

bFGF and cav-1 were the target genes in this study. Tubulin was used as a reference gene

F forward, *R* reverse

electrophoresis in 12% sodium dodecylsulfate-polyacrylamide gels (SDS-PAGE) and then transferred to 0.45-μm PVDF membranes. The membranes were blocked with 5% non-fat milk in Tris-buffered saline with Tween 20 (TBST; Solarbio) at room temperature for 2 h. After blocking, the membranes were incubated overnight at 4 °C with the following primary antibodies: bFGF (SC-79, 1:500, Santa Cruz Biotechnology, Inc.), cav-1 (ab2910, 1:1000, Abcam, UK), VEGF (ab46154, 1:1000, Abcam, UK), and Tubulin (AT819, 1:1000, Beyotime Biotechnology, China). After three washes in TBST, the membranes were incubated with horseradish peroxidase (HRP)-conjugated secondary antibodies (goat anti-mouse IgG, 1:5000, Jackson, USA; goat anti-rabbit IgG, 1:5000, Jackson, USA) for 2 h at room temperature, followed by another three washes. Enhanced chemiluminescence (ECL) reagents (ThermoScientific, Inc.) were used to detect the blots. Signals were collected with a DNR MicroChemi System. The Quantity One software (version 4.6.2; Bio-Rad Laboratories, Inc.) was used to quantify the results. The protein loading control was Tubulin. The relative expression levels of bFGF, cav-1, and VEGF were calculated as a percentage of Tubulin expression.

Immunofluorescence Staining

Astrocytes were fixed with 4% paraformaldehyde (PFA) for 30 min and washed three times with PBS. Next, the astrocytes were incubated with 0.5% Triton X-100 at room temperature for 20 min. Following three washes in PBS, the cells were incubated with 5% bovine serum albumin (BSA) or 10% goat serum at room temperature for 30 min. Then, samples were incubated with anti-GFAP antibody (ab68428, 1:200, Abcam, UK), anti-bFGF antibody (ab8880, 1:200, Abcam, UK), anti-cav-1 antibody (ab2910, 1:500, Abcam, UK), and anti-VEGF antibody (ab46154, 1:50, Abcam, UK) overnight at 4 °C. After three washes in phosphate-buffered saline with Tween 20 (PBST), samples were incubated with Alexa Fluor 594 AffiniPure goat anti-rabbit IgG (33112ES60, 1:200, Yeasen Biotechnology, China) and Alexa Fluor 488 AffiniPure goat anti-rabbit IgG (A-11034, 1:200, ThermoScientific, Inc.) at 37 °C for 1 h, followed by another three washes. The nucleus was stained with DAPI for 5 min at room temperature. Nikon ECLIPSE Timicroscope (Nikon, Tokyo, Japan) was used to capture all images. Image-Pro Plus (IPP) software (version 6.0, Media Cybernetics Inc., USA) was used for quantitative analysis of immunofluorescence staining.

Statistical Analysis of Data

All data were expressed as the mean ± standard error of mean. Prism Software 5.0 (GraphPad Software Inc., San Diego, CA, USA) was used for statistical analysis. Statistical comparisons for different groups (more than two groups) were performed using one-way analysis of variance (ANOVA) followed by post hoc Bonferroni tests. A Student's *t* test was used for comparative analysis between two groups. The correlation analysis of two variables was performed using Pearson product moment correlation analysis. *P* values <0.05 were defined as statistically significant.

Results

Efficiency of bFGF Knockdown in Astrocytes

The efficiency of lentivirus transfection was measured by fluorescent microscopy. Results showed that more than 80% of the astrocytes were successfully transfected by lentivirus (data not shown). RT-qPCR was performed to detect the efficiency of bFGF knockdown. As shown in Fig. 1a, bFGF mRNA expression in the sibFGF group was reduced by 50 ± 8.96 and 43 ± 9.89%, compared with the control group and NC siRNA group, respectively.

RT-qPCR analysis was also performed to study the effect of OGD/R on bFGF mRNA expression and the inhibitory effect of sibFGF on the increased expression of bFGF induced by OGD/R in astrocytes. bFGF mRNA expression levels in the OGD/R group and NC siRNA + OGD/R group were increased by 112 ± 32.4 and 92.4 ± 41.4%, compared with those in the control group and NC siRNA group, respectively.

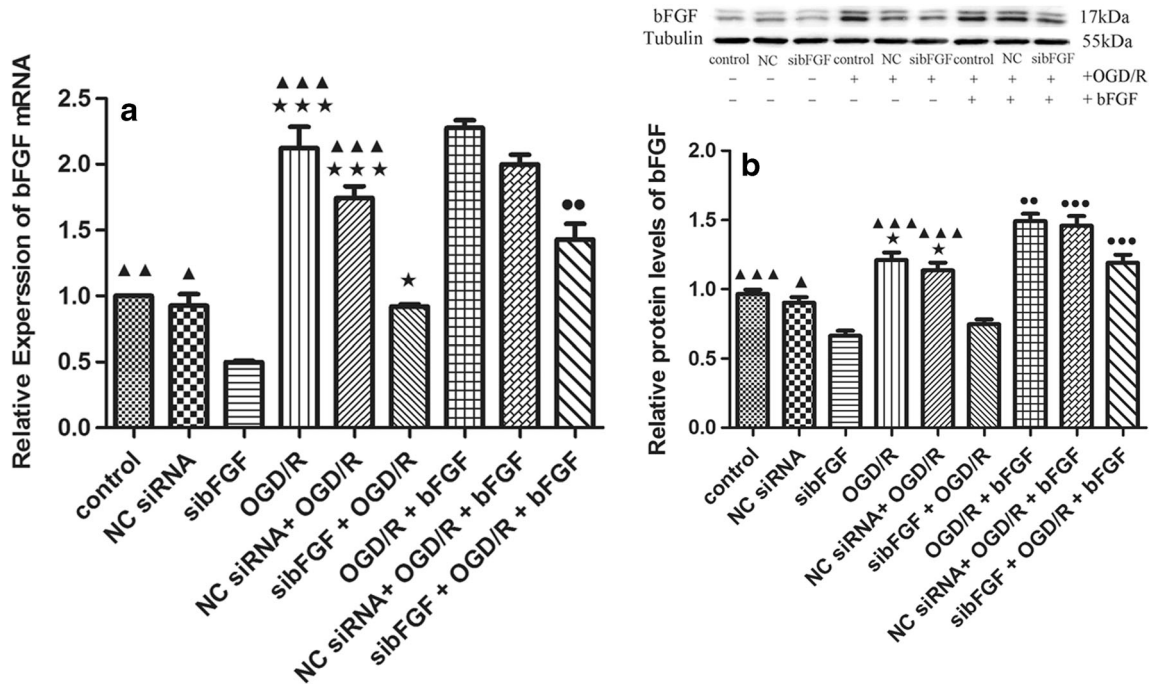

Fig. 1 **a** Relative mRNA expression levels of bFGF in primary astrocytes measured by RT-qPCR. Results were normalized to Tubulin 3 gene expression and expressed as fold change versus the control group. **b** Relative protein expression levels of bFGF in primary astrocytes examined by western blotting. Tubulin was used as the loading control. Values were calculated as a percentage of Tubulin expression and expressed as the relative optical density. ($^{\star}P < 0.05$; $^{\star\star}P < 0.01$; $^{\star\star\star}P < 0.001$ vs. no OGD/R groups, $^{\blacktriangle}P < 0.05$; $^{\blacktriangle\blacktriangle}P < 0.01$; $^{\blacktriangle\blacktriangle\blacktriangle}P < 0.001$ vs. sibFGF groups, $^{\bullet}P < 0.05$; $^{\bullet\bullet}P < 0.01$; $^{\bullet\bullet\bullet}P < 0.001$ vs. no bFGF groups. All data are the mean ± SEM of six independent experiments)

However, treatment with bFGF siRNA abrogated these increases by 55.8 ± 7.7 and 46.2 ± 4.7%, respectively. In addition, under OGD/R conditions, treatment with bFGF siRNA and exogenous bFGF concurrently increased the bFGF mRNA expression levels by 53.1 ± 19.2%, compared with astrocytes treated with bFGF siRNA alone. These results suggested that OGD/R obviously elevated the mRNA expression levels of bFGF, which were effectively inhibited by bFGF knockdown, and that decreased bFGF mRNA expression levels by bFGF knockdown were efficiently reversed by exogenous bFGF. Furthermore, compared with astrocytes in the OGD/R group and NC siRNA + OGD/R group, exogenous treatment with bFGF increased the bFGF mRNA expression levels by 8.7 ± 12.6 and 15.4 ± 12.8%, respectively, although this was not significantly different (Fig. 1a).

We also measured the protein expression levels of bFGF by western blot analysis, which showed that the protein levels of bFGF in the OGD/R group and NC siRNA + OGD/R group were increased by 26.2 ± 20.7 and 26.7 ± 17.3%, compared with those in the control group and NC siRNA group, respectively. This effect was abolished by pre-treatment with bFGF siRNA (38.1 ± 5.4 and 33.8 ± 7.5%, respectively), and the decreased protein levels of bFGF by bFGF knockdown were reversed by 62.7 ± 35.0% by treatment with exogenous bFGF. These results were consistent with the RT-qPCR results. However, there was a significant difference in protein levels of bFGF between the OGD/R + bFGF group and OGD/R group (increased by 25.1 ± 20.0%) as well as between the NC siRNA + OGD/R + bFGF group and NC siRNA + OGD/R group (increased by 30.7 ± 26.7%), which was different from the RT-qPCR results (Fig. 1b). As shown in Fig. 2, the results of immunofluorescence staining for bFGF were consistent with the western blotting results.

bFGF Knockdown Decreases Cell Viability of Astrocyte after OGD/R

To investigate the effect of bFGF on the survival of astrocytes after OGD/R, a CCK-8 assay was performed. The results of the CCK-8 assay (Fig. 3a) demonstrated that the cell viability of astrocytes in the OGD/R group and NC siRNA + OGD/R group was markedly reduced compared with that in the control group and NC siRNA group (0.69 ± 0.12 versus 1.00 ± 0.00; 0.59 ± 0.08 versus 0.91 ± 0.13, respectively). The cell viability of astrocytes pre-treated with bFGF siRNA prior to OGD/R was decreased compared with that in the OGD/R group and NC siRNA + OGD/R group (0.39 ± 0.08 versus 0.69 ± 0.12 and 0.59 ± 0.08, respectively). However, the cell viability of astrocytes in the sibFGF + OGD/R + bFGF group was significantly increased compared with that in the sibFGF + OGD/R group (0.62 ± 0.04 versus 0.39 ± 0.08). These results indicated that the cell damage in astrocytes

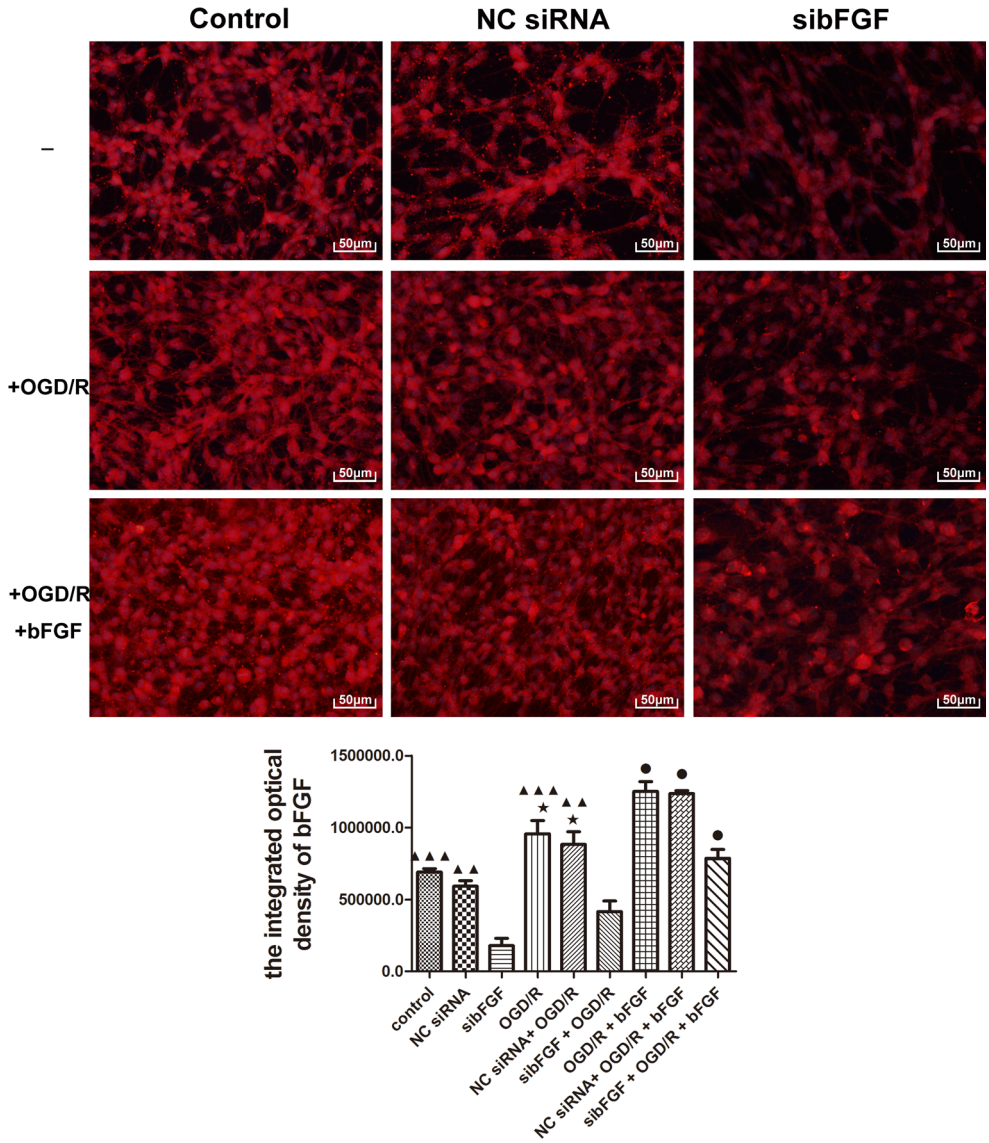

Fig. 2 *Upper* immunofluorescence staining for bFGF. First column, astrocytes without treatment; second column, astrocytes transfected with NC siRNA; third column, astrocytes transfected with sibFGF; first line, astrocytes cultured under normoxic conditions; second line, astrocytes subjected to OGD/R; third line, astrocytes pre-treated with exogenous bFGF prior to OGD/R. Red represents bFGF, blue represents DAPI. Scale bar is 50 μm. *Lower* quantitative analysis of bFGF immunofluorescence staining. Fluorescence intensity was calculated by the integrated optical density. $^{\star}P < 0.05$; $^{\star\star}P < 0.01$; $^{\star\star\star}P < 0.001$ vs. no OGD/R groups, $^{\blacktriangle}P < 0.05$; $^{\blacktriangle\blacktriangle}P < 0.01$; $^{\blacktriangle\blacktriangle\blacktriangle}P < 0.001$ vs. sibFGF groups, $^{\bullet}P < 0.05$; $^{\bullet\bullet}P < 0.01$; $^{\bullet\bullet\bullet}P < 0.001$ vs. no bFGF groups. All data are the mean ± SEM of five independent experiments

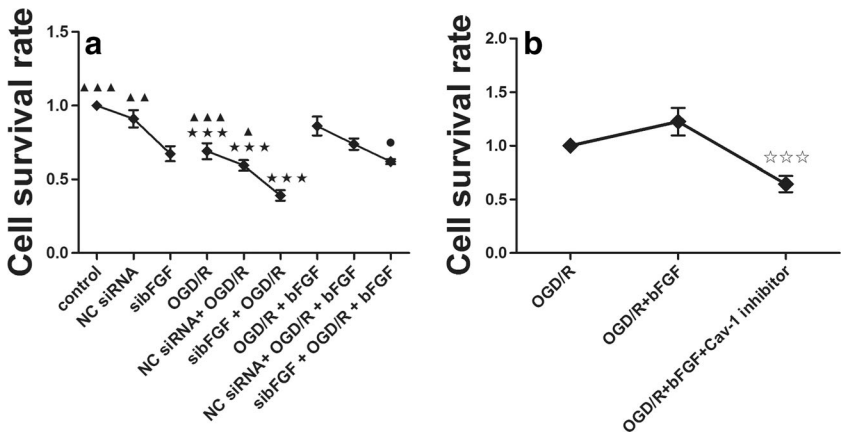

Fig. 3 **a**. The effects of OGD/R, bFGF knockdown and exogenous bFGF protein on cell survival rate of astrocytes evaluated by CCK-8 assay. $^{\star}P < 0.05$, $^{\star\star}P < 0.01$, $^{\star\star\star}P < 0.001$ vs. no OGD/R groups; $^{\blacktriangle}P < 0.05$, $^{\blacktriangle\blacktriangle}P < 0.01$, $^{\blacktriangle\blacktriangle\blacktriangle}P < 0.001$ vs. sibFGF groups; $^{\bullet}P < 0.05$, $^{\bullet\bullet}P < 0.01$, $^{\bullet\bullet\bullet}P < 0.001$ vs. no bFGF groups. **b**. The effect of cav-1 inhibitor on cell survival rate of astrocytes evaluated by CCK-8 assay. $^{\star}P < 0.05$, $^{\star\star}P < 0.01$, $^{\star\star\star}P < 0.001$ vs. OGD/R+bFGF group. (All data are the mean ± SEM of five independent experiments)

following OGD/R was aggravated by bFGF knockdown; however, it was reduced by exogenous bFGF. Moreover, the cell viability of astrocytes in the OGD/R + bFGF group and NC siRNA + OGD/R + bFGF group was increased compared with that in the OGD/R group and NC siRNA + OGD/R group, but both were not significantly different (0.86 ± 0.14 versus 0.69 ± 0.12; 0.74 ± 0.09 versus 0.59 ± 0.08, respectively).

To investigate whether bFGF affected cell viability via the cav-1 signaling pathway, we performed another experiment, which showed that the cell viability of astrocytes in the OGD/R + bFGF + cav-1 inhibitor group was significantly reduced (0.64 ± 0.20 versus 1.23 ± 0.34), compared with that in the OGD/R + bFGF group (Fig. 3b).

bFGF Knockdown Inhibits Increases in cav-1 and VEGF Expression Following OGD/R

RT-qPCR, western blotting, and immunofluorescence staining were performed to study the association between bFGF, cav-1, and VEGF.

The RT-qPCR results showed that OGD/R enhanced the mRNA expression levels of cav-1 in the control group and NC siRNA group by 185.4 ± 74.9 and 160.3 ± 77.9%, respectively, which were partly abrogated by bFGF knockdown (33.0 ± 16.3 and 35.8 ± 30.9%, respectively), and the decreased cav-1 mRNA expression levels by bFGF knockdown were reversed by 55.0 ± 61.1% by treatment with exogenous bFGF. Furthermore, cav-1 mRNA expression levels in the OGD/R + bFGF group and NC siRNA + OGD/R + bFGF group were increased by 41.1 ± 45.1 and 29.7 ± 37.2%, compared with those in the OGD/R group and NC siRNA + OGD/R group, respectively (Fig. 4a).

The results of western blotting showed that OGD/R increased the protein levels of cav-1 (by 50.3 ± 34.7 and 45.8 ± 28.0%, respectively) and VEGF (by 54.3 ± 30.9 and 41.2 ± 28.0%, respectively) in the control group and NC siRNA group, which were abolished by treatment with bFGF siRNA (cav-1, 30.9 ± 14.7 and 21.8 ± 12.5%, respectively; VEGF, 39.9 ± 15.0 and 28.8 ± 13.2%, respectively), and the decreased protein levels of cav-1 and VEGF by bFGF knockdown were reversed (cav-1, 45.4 ± 31.8; VEGF, 47.5 ± 35.4%) by treatment with exogenous bFGF. Moreover, the protein levels of cav-1 and VEGF in the OGD/R + bFGF group and NC siRNA + OGD/R + bFGF group were both increased (cav-1, by 27.5 ± 24.0 and 39.0 ± 32.8%; VEGF, by 30.5 ± 18.6 and 41.8 ± 26.1%), compared with those in the OGD/R group and NC siRNA + OGD/R group, respectively (Fig. 4b, c). Furthermore, immunofluorescence staining for cav-1 and VEGF was consistent with the western blotting results (Figs. 5 and 6).

These results suggested that the increased expression of bFGF induced by OGD/R elevated cav-1 and VEGF expression, and bFGF knockdown inhibited the increased cav-1 and VEGF expression following OGD/R; however, exogenous bFGF rescued the effect of bFGF knockdown on cav-1 and VEGF expression under OGD/R conditions.

To clarify whether the expression of cav-1 and VEGF were closely related to bFGF expression, a correlation analysis between them was performed. Pearson product moment correlation analysis was used, which showed a significant positive correlation between bFGF protein expression and cav-1 protein expression ($r = 0.8492$, $P < 0.01$, $n = 54$), between bFGF protein expression and VEGF protein expression ($r = 0.7559$, $P < 0.01$, $n = 54$), and between bFGF mRNA expression and cav-1 mRNA expression ($r = 0.7320$, $P < 0.01$, $n = 54$). Of note, western blotting was used to perform correlation analysis of the protein expression between bFGF and cav-1 as well as between bFGF and VEGF (data was not shown).

cav-1 Inhibitor Abolished the Effect of bFGF on VEGF Expression in Astrocytes under OGD/R Conditions

Based on the above, we performed another experiment using a cav-1 inhibitor. As shown in Fig. 7, the protein expression levels of cav-1 and VEGF in the OGD/R + bFGF + cav-1 inhibitor group were decreased (cav-1, by 39.0 ± 17.6%; VEGF, by 25.2 ± 5.9%), compared with those in the OGD/R + bFGF group. However, there was no significant difference between the protein expression levels of bFGF in the OGD/R + bFGF + cav-1 inhibitor group and the OGD/R + bFGF group.

Discussion

Cerebral ischemia has a high disability and mortality rate. Recent studies have concentrated on the self-remodeling of brain tissue and functional recovery after ischemia. In this study, we found that bFGF expression was markedly increased in primary astrocytes subjected to OGD/R injury, which resulted in the higher expression of cav-1 and VEGF. In contrast, bFGF knockdown not only significantly reduced the expression of bFGF, but also markedly decreased the expression of cav-1 and VEGF in OGD/R astrocytes. However, exogenous treatment with bFGF reversed the decreased expression of bFGF, cav-1, and VEGF in sibFGF + OGD/R astrocytes. Moreover, exogenous bFGF treatment significantly increased the expression of cav-1 and VEGF in OGD/R astrocytes. These results suggested that bFGF positively modulates cav-1 and VEGF expression in astrocytes under hypoxic conditions. We also found that a cav-1 inhibitor significantly reduced VEGF expression in astrocytes pre-treated with 20 ng/ml bFGF prior to OGD/R, which indicated that the cav-1 inhibitor abolished the effect of bFGF on VEGF expression. Thus, cav-1 mediated the effect of bFGF on VEGF

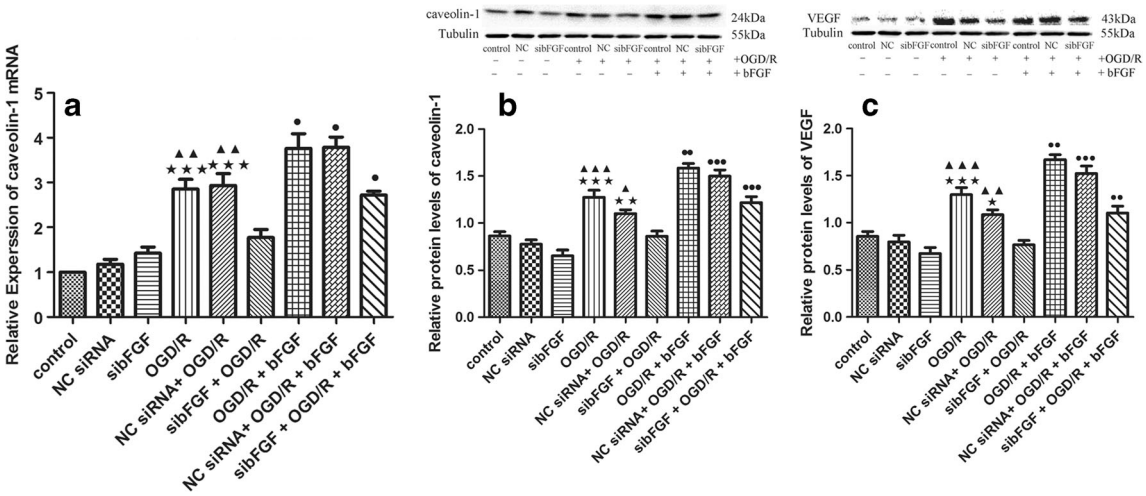

Fig. 4 **a** Relative mRNA expression levels of cav-1 in primary astrocytes measured by RT-qPCR. Results were normalized to Tubulin 3 gene expression and expressed as fold change versus the control group. Relative protein expression levels of cav-1 (**b**) and VEGF (**c**) in primary astrocytes examined by western blotting. Tubulin was used as the loading control. Values were calculated as a percentage of Tubulin expression and expressed as the relative optical density. ($^{\star}P < 0.05$; $^{\star\star}P < 0.01$; $^{\star\star\star}P < 0.001$ vs. no OGD/R groups, $^{\blacktriangle}P < 0.05$; $^{\blacktriangle\blacktriangle}P < 0.01$; $^{\blacktriangle\blacktriangle\blacktriangle}P < 0.001$ vs. sibFGF groups, $^{\bullet}P < 0.05$; $^{\bullet\bullet}P < 0.01$; $^{\bullet\bullet\bullet}P < 0.001$ vs. no bFGF groups. All data are the mean ± SEM of six independent experiments)

expression in astrocytes under hypoxic conditions. The results of the CCK-8 assay in this study showed that bFGF knockdown aggravated the injury of OGD/R on primary astrocytes; however, restoring bFGF by exogenous bFGF treatment improved the survival of astrocytes. A study performed by Qiao et al. (2016) showed that bFGF significantly attenuated hypoxia-induced apoptosis in bone marrow-derived mesenchymal stromal cells (BMSCs). These results indicated that bFGF has a protective role in cell injury. Furthermore, a cav-1 inhibitor abrogated the effect of bFGF on the cell viability of astrocytes. Therefore, we suggest that bFGF may protect astrocytes from OGD/R-induced injury by upregulating the caveolin-1/VEGF signaling pathway.

Recent studies have shown that bFGF is upregulated and plays an indispensable role in the proliferation and differentiation of stem cells after ischemic insults (Yang et al. 2014), especially NSPCs in the SVZ of the lateral ventricles and CVOs (Lin et al. 2015). bFGF expression is also induced under many other injury conditions, such as spinal cord injury (Jia et al. 2014) and trauma (Rotschafer et al. 2013; Xiang et al. 2014), and is beneficial for functional recovery. Our previous in vivo studies found that the intracerebroventricular injection of exogenous bFGF protein in a MCAO rat decreased cerebral infarct volume, promoted neurological recovery, and facilitated angiogenesis and neurogenesis through upregulating the caveolin-1/VEGF signaling pathway (Gao et al. 2014; Zhao et al. 2017). This present in vitro study preliminarily demonstrated that bFGF protected astrocytes from injury induced by OGD/R via the caveolin-1/VEGF signaling pathway. Thus, we suggest bFGF may play a crucial role after cerebral ischemic injury partly by upregulating the caveolin-1/VEGF signaling pathway in astrocytes. In addition to the roles of the caveolin-1/VEGF signaling pathway in angiogenesis and neurogenesis, it may be also involved in astrogliosis, astroglial scar formation and neuroinflammation after cerebral ischemia. Studies have demonstrated that neutralizing antibodies to VEGFR1, which is predominantly expressed by astrocytes in the CNS, or the downregulation of VEGF significantly decreased the formation of reactive astrocytes and gliosis after cerebral ischemia (Krum et al. 2008; Na et al. 2015). In addition, cav-1 was reported to suppress neuroinflammatory responses in ischemic stroke by directly interacting with Toll-like receptor 4 (Niesman et al. 2014; Xu et al. 2016). Xu et al. (2017) reported that VEGF suppressed neuroinflammation and ischemic brain injury by inhibiting SR-A expression. Thus, further research is required.

cav-1 is a multifunctional membrane protein that has an important role in regulating cell functions, including cellular repair after stroke (Liu et al. 2002; Mundy et al. 2002; Navarro et al. 2004). Studies performed by Head et al. (2008) and Jasmin et al. (2007) showed that cav-1 protected neurons from ischemic injury through the NMDAR/SFK/ERK1/2 signaling pathway, and that cav-1 plays an active role in regulating synaptic remodeling after injury in the CNS (Gaudreault et al. 2005). Several studies also showed that cav-1 gene ablation in mice leads to increased cerebral infarction volume, increased cell death, and impaired angiogenesis (Chidlow and Sessa 2010; Jasmin et al. 2007). These studies suggest that cav-1 functions as a positive regulator participating in the functional recovery of cerebral ischemic stroke. However, some studies reported that cav-1 has a negative role in neurogenesis and/or neuroprotection. For example, cav-1 gene ablation increased the proliferation of neural stem cells in the SVZ of adult mouse brain (Jasmin et al. 2009). cav-1

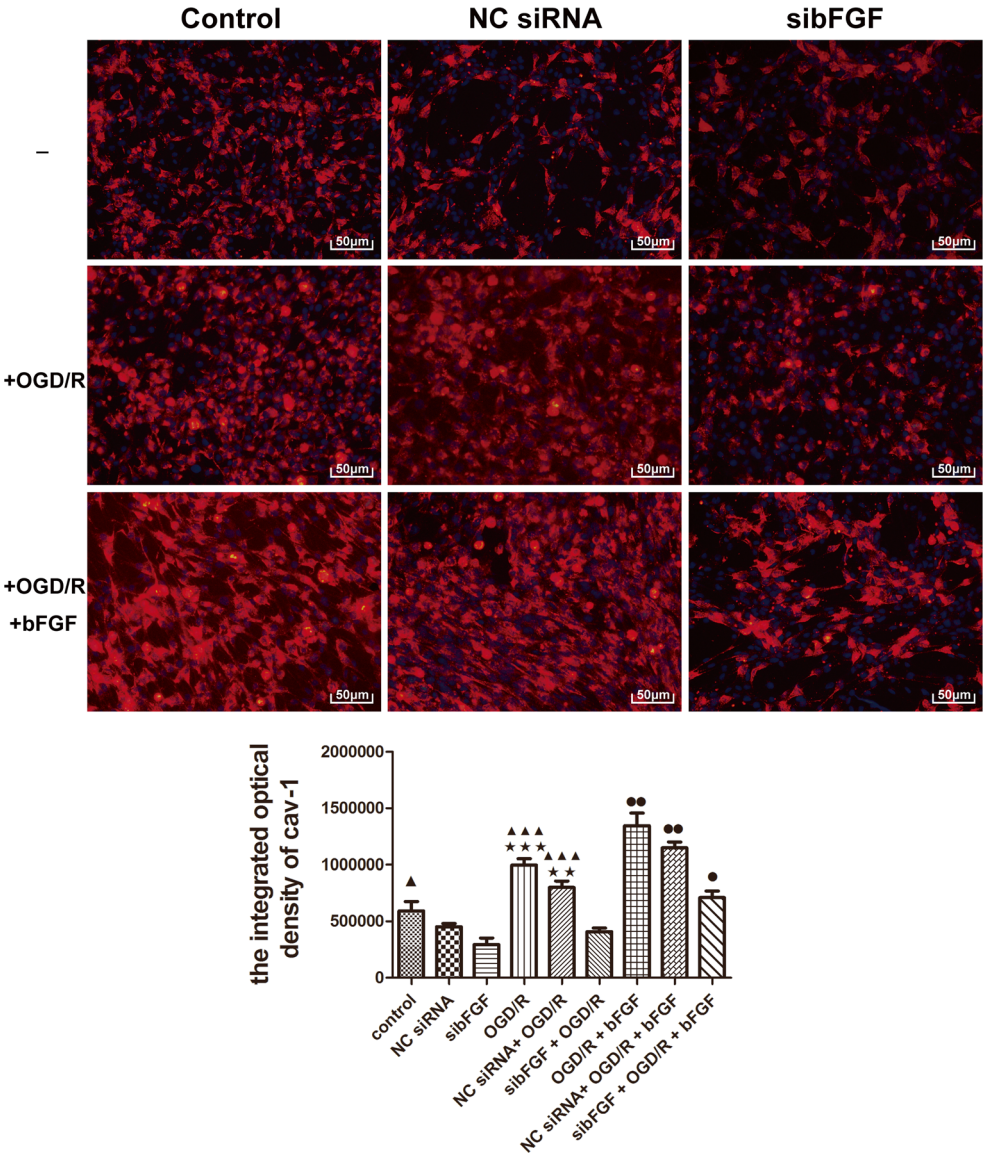

Fig. 5 *Upper* immunofluorescence staining for cav-1. Red represents cav-1, blue represents DAPI, and the scale bar is 50 μm. *Lower* quantitative analysis of cav-1 immunofluorescence staining. Fluorescence intensity was calculated by the integrated optical density. $^{\star}P < 0.05$; $^{\star\star}P < 0.01$; $^{\star\star\star}P < 0.001$ vs. no OGD/R groups, $^{\blacktriangle}P < 0.05$; $^{\blacktriangle\blacktriangle}P < 0.01$; $^{\blacktriangle\blacktriangle\blacktriangle}P < 0.001$ vs. sibFGF groups, $^{\bullet}P < 0.05$; $^{\bullet\bullet}P < 0.01$; $^{\bullet\bullet\bullet}P < 0.001$ vs. no bFGF groups. All data are the mean ± SEM of five independent experiments

inhibited the neuronal differentiation of NSPCs through the downregulation of VEGF and the p44/42MAPK signaling pathway (Li et al. 2011), and cav-1 blocked the formation and growth of neurites (Kang et al. 2006). One explanation might be that, in the present study, we selected rat astrocytes as the experimental subject, and the mechanisms of action of cav-1 may be different in various cells and/or under different conditions, such as hypoxia and normoxia.

The mechanisms of the upregulation of the caveolin-1/VEGF signaling pathway by bFGF in astrocytes under hypoxic conditions are unclear. Studies have shown that hypoxia-induced VEGF expression is directly regulated by hypoxia inducible factor 1 (HIF-1), a heterodimeric transcription factor comprised of an α subunit and a constitutively expressed β subunit. Shi et al. (2007, 2005) found that bFGF augmented hypoxia-induced HIF-1α and VEGF expression through the MEK1/ERK and PI3K/Akt signaling pathways, which was abrogated by a FGFR1 inhibitor. This indicated that FGFR1 mediates the effects of bFGF. Studies performed by Feng et al. (2012) and Ye et al. (2016) reported cav-1 was involved in the regulation of FGFR1, largely owing to their co-localization on cell membranes. The study by Ye et al. (2016) also showed that bFGF treatment did not reverse the inhibitory effect of cav-1 siRNA on FGFR1 expression and its co-localization with cav-1. Thus, we suggest an interaction between cav-1 and FGFR1 might be essential for the protective effect of bFGF in astrocytes, but the interaction mechanism of cav-1 and FGFR1 needs to be studied further. In this study, we found that downregulation of endogenous bFGF and the addition of recombinant bFGF, respectively, reduced and increased the expression of cav-1 and VEGF in OGD/R astrocytes, which indicates that cav-1 and VEGF expression are modulated by endogenous bFGF as well as by exogenous bFGF under hypoxic conditions. Considering the autocrine function of bFGF

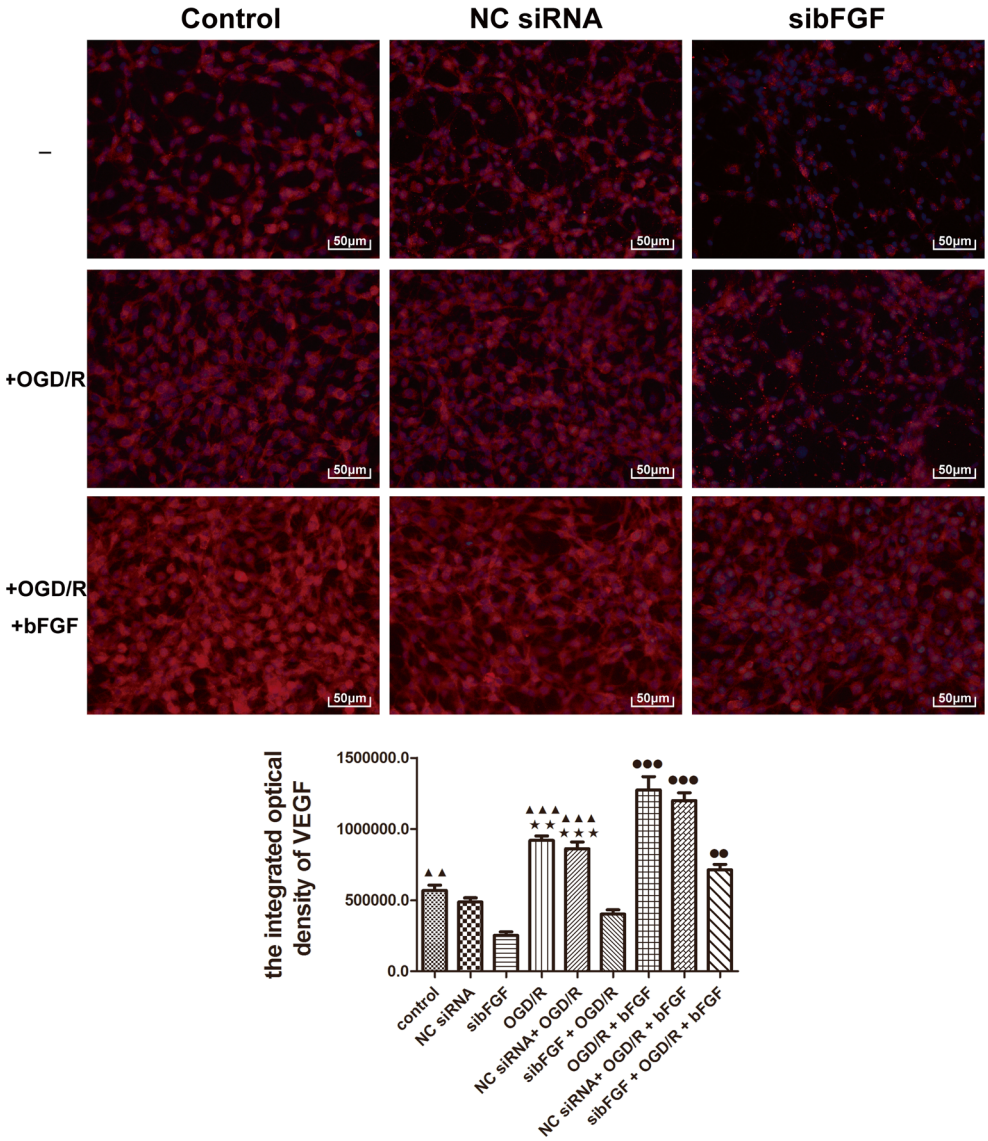

Fig. 6 *Upper* Immunofluorescence staining for VEGF. Red represents VEGF, blue represents DAPI, and the scale bar is 50 μm. *Lower* quantitative analysis of VEGF immunofluorescence staining. Fluorescence intensity was calculated by the integrated optical density. $^{\star}P < 0.05$; $^{\star\star}P < 0.01$; $^{\star\star\star}P < 0.001$ vs. no OGD/R groups, $^{\blacktriangle}P < 0.05$; $^{\blacktriangle\blacktriangle}P < 0.01$; $^{\blacktriangle\blacktriangle\blacktriangle}P < 0.001$ vs. sibFGF groups, $^{\bullet}P < 0.05$; $^{\bullet\bullet}P < 0.01$; $^{\bullet\bullet\bullet}P < 0.001$ vs. no bFGF groups. All data are the mean ± SEM of five independent experiments

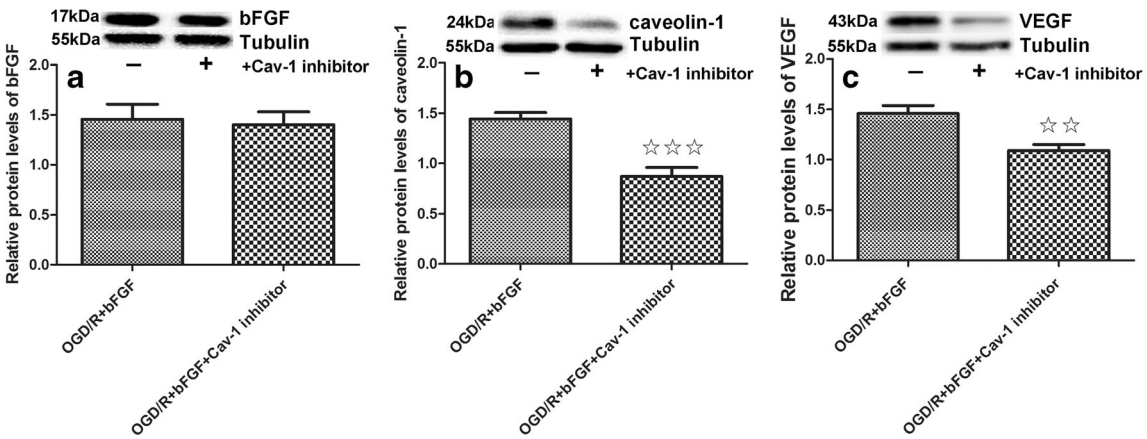

Fig. 7 Relative protein expression levels of bFGF (**a**), cav-1 (**b**), and VEGF (**c**) in primary astrocytes examined by western blotting. Tubulin was used as the loading control. Values were calculated as a percentage of Tubulin expression and expressed as the relative optical density. $^{\star}P < 0.05$; $^{\star\star}P < 0.01$; $^{\star\star\star}P < 0.001$ vs. OGD/R + bFGF group. All data are the mean ± SEM of nine independent experiments

(Seghezzi et al. 1998), we believe that the upregulation of cav-1 and VEGF expression by endogenous bFGF requires the release of bFGF from cells and interactions with cell membrane receptors such as FGFR1. A recent study demonstrated that a low concentration of bFGF, from 10 to 50 ng/mL, induced the activation of astrocytes via the regulation of the TLR4/NF-κB signaling pathway, which in turn enhanced endogenous bFGF expression in vitro (Ye et al. 2015). This may be why bFGF expression was increased in all bFGF-treated groups under OGD/R conditions. Of note, bFGF mRNA expression was increased in astrocytes pre-treated with 20 ng/ml bFGF prior to OGD/R, compared with that in OGD/R astrocytes, although this was not significantly different. Studies have shown that mRNA stability often opposes transcription, that is, mRNAs with high transcription levels are not stable (de Sousa Abreu et al. 2009). The transcription levels in the sibFGF + OGD/R + bFGF group may be lower than those in the OGD/R + bFGF group or NC siRNA + OGD/R + bFGF group; thus, bFGF mRNA in the sibFGF + OGD/R + bFGF group may be more stable than that in the OGD/R + bFGF group or NC siRNA + OGD/R + bFGF group. This may explain why exogenous bFGF increased bFGF mRNA levels in the sibFGF + OGD/R + bFGF group, but did not increase levels of bFGF mRNA in the OGD/R + bFGF group and the NC siRNA + OGD/R + bFGF group.

Many other signaling molecules may take part in the mechanisms of bFGF after cerebral I/R injury. For instance, high-mobility group box 1 (HMGB1), which is mainly released from astrocytes, promoted neurovascular remodeling during stroke recovery by activating endothelial progenitor cells (EPCs) (Hayakawa et al. 2012) and upregulating VEGF expression (Biscetti et al. 2010). In addition, studies reported that cav-1 increased the expression of HMGB1 (Wang et al. 2014). Thus, further experiments are necessary to clarify the complex regulatory mechanisms of bFGF involved in stroke recovery.

Acknowledgments We appreciate the great technical support provided by the Laboratory Center of the Second Affiliated Hospital & Yuying Children's Hospital of Wenzhou Medical University and the Experimental Animal Center of Wenzhou Medical University.

Funding This study was supported partially by the research funding from the Chinese Ministry of Health Project (No. 201302002 to XC) and the Natural Science Foundation of Zhejiang Province Project (No. Y12H170002).

Compliance with Ethical Standards This study was approved by the Ethics Committee of Wenzhou Medical University.

Conflict of Interest We certify that all authors have no financial or other conflict of interests in connection with the submitted article.

Abbreviations *bFGF*, basic fibroblast growth factor; *cav-1*, caveolin-1; *CNS*, central nervous system; *Cq*, quantification cycle; *GFAP*, glial fibrillary acidic protein; *HIF-1α*, hypoxia inducible factor 1α; *I/R*, ischemia/reperfusion; *MCAO*, middle cerebral artery occlusion; *MOI*, multiplicity of infection; *NSPCs*, neural stem/progenitor cells; *OD*, optical density; *OGD/R*, oxygen glucose deprivation/reoxygenation; *PBS*, Phosphate Buffered Saline; *RT-qPCR*, reverse transcription-quantitative polymerase chain reaction; *SVZ*, subventricular zone; *VEGF*, vascular endothelial growth factor

References

Basilico C, Moscatelli D (1992) The FGF family of growth factors and oncogenes. Adv Cancer Res 59:115–165. https://doi.org/10.1016/S0065-230X(08)60305-X

Bethel A, Kirsch JR, Koehler RC, Finklestein SP, Traystman RJ (1997) Intravenous basic fibroblast growth factor decreases brain injury resulting from focal ischemia in cats. Stroke 28(3):609–616. https://doi.org/10.1161/01.str.28.3.609

Biscetti F, Straface G, De Cristofaro R, Lancellotti S, Rizzo P, Arena V, Stigliano E, Pecorini G, Egashira K, De Angelis G, Ghirlanda G, Flex A (2010) High-mobility group box-1 protein promotes angiogenesis after peripheral ischemia in diabetic mice through a VEGF-dependent mechanism. Diabetes 59(6):1496–1505. https://doi.org/10.2337/db09-1507

Chidlow JH Jr, Sessa WC (2010) Caveolae, caveolins, and cavins: complex control of cellular signalling and inflammation. Cardiovasc Res 86(2):219–225. https://doi.org/10.1093/cvr/cvq075

de Sousa AR, Penalva LO, Marcotte EM, Vogel C (2009) Global signatures of protein and mRNA expression levels. Mol BioSyst 5:1512–1526. https://doi.org/10.1039/b908315d

Feng L, Liao WX, Luo Q, Zhang HH, Wang W, Zheng J, Chen DB (2012) Caveolin-1 orchestrates fibroblast growth factor 2 signaling control of angiogenesis in placental artery endothelial cell caveolae. J Cell Physiol 227(6):2480–2491. https://doi.org/10.1002/jcp.22984

Gao Y, Zhao Y, Pan J, Yang L, Huang T, Feng X, Li C, Liang S, Zhou D, Liu C, Tu F, Tao C, Chen X (2014) Treadmill exercise promotes angiogenesis in the ischemic penumbra of rat brains through caveolin-1/VEGF signaling pathways. Brain Res 1585:83–90. https://doi.org/10.1016/j.brainres.2014.08.032

Gaudreault SB, Blain JF, Gratton JP, Poirier J (2005) A role for caveolin-1 in post-injury reactive neuronal plasticity. J Neurochem 92(4):831–839. https://doi.org/10.1111/j.1471-4159.2004.02917.x

Hansen TM, Moss AJ, Brindle NP (2008) Vascular endothelial growth factor and angiopoietins in neurovascular regeneration and protection following stroke. Curr Neurovasc Res 5(4):236–245. https://doi.org/10.2174/156720208786413433

Hayakawa K, Pham LD, Katusic ZS, Arai K, Lo EH (2012) Astrocytic high-mobility group box 1 promotes endothelial progenitor cell-mediated neurovascular remodeling during stroke recovery. Proc Natl Acad Sci U S A 109(19):7505–7510. https://doi.org/10.1073/pnas.1121146109

Head BP, Patel HH, Tsutsumi YM, Hu Y, Mejia T, Mora RC, Insel PA, Roth DM, Drummond JC, Patel PM (2008) Caveolin-1 expression is essential for *N*-methyl-D-aspartate receptor-mediated Src and extracellular signal-regulated kinase 1/2 activation and protection of primary neurons from ischemic cell death. FASEB J 22(3):828–840. https://doi.org/10.1096/fj.07-9299com

Jang S, Cho HH, Cho YB, Park JS, Jeong HS (2010) Functional neural differentiation of human adipose tissue-derived stem cells using bFGF and forskolin. BMC Cell Biol 11(1):25. https://doi.org/10.1186/1471-2121-11-25

Jasmin JF, Malhotra S, Singh Dhallu M, Mercier I, Rosenbaum DM, Lisanti MP (2007) Caveolin-1 deficiency increases cerebral ischemic injury. Circ Res 100(5):721–729. https://doi.org/10.1161/01.RES.0000260180.42709.29

Jasmin JF, Yang M, Iacovitti L, Lisanti MP (2009) Genetic ablation of caveolin-1 increases neural stem cell proliferation in the subventricular zone (SVZ) of the adult mouse brain. Cell Cycle 8(23):3978–3983. https://doi.org/10.4161/cc.8.23.10206

Jia Y, Wu D, Zhang R, Shuang W, Sun J, Hao H, An Q, Liu Q (2014) Bone marrow-derived mesenchymal stem cells expressing the Shh transgene promotes functional recovery after spinal cord injury in rats. Neurosci Lett 573:46–51. https://doi.org/10.1016/j.neulet.2014.05.010

Kalluri HS, Dempsey RJ (2008) Growth factors, stem cells, and stroke. Neurosurg Focus 24(3-4):E14. https://doi.org/10.3171/FOC/2008/24/3-4/E13

Kang MJ, Seo JS, Park WY (2006) Caveolin-1 inhibits neurite growth by blocking Rac1/Cdc42 and p21-activated kinase 1 interactions. Neuroreport 17(8):823–827. https://doi.org/10.1097/01.wnr.0000220139.83671.60

Kang ML, Kwon JS, Kim MS (2013) Induction of neuronal differentiation of rat muscle-derived stem cells in vitro using basic fibroblast growth factor and ethosuximide. Int J Mol Sci 14(4):6614–6623. https://doi.org/10.3390/ijms14046614

Koyama Y, Maebara Y, Hayashi M, Nagae R, Tokuyama S, Michinaga S (2012) Endothelins reciprocally regulate VEGF-A and angiopoietin-1 production in cultured rat astrocytes: implications on astrocytic proliferation. Glia 60(12):1954–1963. https://doi.org/10.1002/glia.22411

Krum JM, Mani N, Rosenstein JM (2008) Roles of the endogenous VEGF receptors flt-1 and flk-1 in astroglial and vascular remodeling after brain injury. Exp Neurol 212(1):108–117. https://doi.org/10.1016/j.expneurol.2008.03.019

Lafuente JV, Ortuzar N, Bengoetxea H, Bulnes S, Argandona EG (2012) Vascular endothelial growth factor and other angioglioneurins: key molecules in brain development and restoration. Int Rev Neurobiol 102:317–346. https://doi.org/10.1016/B978-0-12-386986-9.00012-0

Lee HJ, Park J, Yoon OJ, Kim HW, Lee DY, do Kim H, Lee WB, Lee NE, Bonventre JV, Kim SS (2011) Amine-modified single-walled carbon nanotubes protect neurons from injury in a rat stroke model. Nat Nanotechnol 6(2):121–125. https://doi.org/10.1038/nnano.2010.281

Li M, Sun L, Li Y, Xie C, Wan D, Luo Y (2014) Oxygen glucose deprivation/reperfusion astrocytes promotes primary neural stem/progenitor cell proliferation by releasing high-mobility group box 1. Neurochem Res 39(8):1440–1450. https://doi.org/10.1007/s11064-014-1333-z

Li Y, Luo J, Lau WM, Zheng G, Fu S, Wang TT, Zeng HP, So KF, Chung SK, Tong Y, Liu K, Shen J (2011) Caveolin-1 plays a crucial role in inhibiting neuronal differentiation of neural stem/progenitor cells via VEGF signaling-dependent pathway. PLoS One 6(8):e22901. https://doi.org/10.1371/journal.pone.0022901

Li YC, Lin YC, Young TH (2012) Combination of media, biomaterials and extracellular matrix proteins to enhance the differentiation of neural stem/precursor cells into neurons. Acta Biomater 8(8):3035–3048. https://doi.org/10.1016/j.actbio.2012.04.036

Li YC, Tsai LK, Young TH (2016) Intraventricular infusion of a low fraction of serum enhances neurogenesis and improves recovery in a rodent stroke model. Neurosci Lett 611:14–20. https://doi.org/10.1016/j.neulet.2015.11.020

Lin R, Cai J, Nathan C, Wei X, Schleidt S, Rosenwasser R, Iacovitti L (2015) Neurogenesis is enhanced by stroke in multiple new stem cell niches along the ventricular system at sites of high BBB permeability. Neurobiol Dis 74:229–239. https://doi.org/10.1016/j.nbd.2014.11.016

Liu P, Rudick M, Anderson RG (2002) Multiple functions of caveolin-1. J Biol Chem 277(44):41295–41298. https://doi.org/10.1074/jbc.R200020200

Lv Y, Zhang B, Zhai C, Qiu J, Zhang Y, Yao W, Zhang C (2015) PFKFB3-mediated glycolysis is involved in reactive astrocyte proliferation after oxygen-glucose deprivation/reperfusion and is regulated by Cdh1. Neurochem Int 91:26–33. https://doi.org/10.1016/j.neuint.2015.10.006

Ma Y, Zechariah A, Qu Y, Hermann DM (2012) Effects of vascular endothelial growth factor in ischemic stroke. J Neurosci Res 90(10):1873–1882. https://doi.org/10.1002/jnr.23088

McCarthy KD, de Vellis J (1980) Preparation of separate astroglial and oligodendroglial cell cultures from rat cerebral tissue. J Cell Biol 85(3):890–902. https://doi.org/10.1083/jcb.85.3.890

Mundy DI, Machleidt T, Ying YS, Anderson RG, Bloom GS (2002) Dual control of caveolar membrane traffic by microtubules and the actin cytoskeleton. J Cell Sci 115(22):4327–4339. https://doi.org/10.1242/jcs.00117

Na JI, Na JY, Choi WY, Lee MC, Park MS, Choi KH, Lee JK, Kim KT, Park JT, Kim HS (2015) The HIF-1 inhibitor YC-1 decreases reactive astrocyte formation in a rodent ischemia model. Am J Transl Res 7(4):751–760

Navarro A, Anand-Apte B, Parat MO (2004) A role for caveolae in cell migration. FASEB J 18(15):1801–1811. https://doi.org/10.1096/fj.04-2516rev

Niesman IR, Schilling JM, Shapiro LA, Kellerhals SE, Bonds JA, Kleschevnikov AM, Cui W, Voong A, Krajewski S, Ali SS, Roth DM, Patel HH, Patel PM, Head BP (2014) Traumatic brain injury enhances neuroinflammation and lesion volume in caveolin deficient mice. J Neuroinflammation 11(1):39. https://doi.org/10.1186/1742-2094-11-39

Noureddini M, Verdi J, Mortazavi-Tabatabaei SA, Sharif S, Azimi A, Keyhanvar P, Shoae-Hassani A (2012) Human endometrial stem cell neurogenesis in response to NGF and bFGF. Cell Biol Int 36(10):961–966. https://doi.org/10.1042/CBI20110610

Pignataro G, Ziaco B, Tortiglione A, Gala R, Cuomo O, Vinciguerra A, Lapi D, Mastantuono T, Anzilotti S, D'Andrea LD, Pedone C, di Renzo G, Annunziato L, Cataldi M (2015) Neuroprotective effect of VEGF-mimetic peptide QK in experimental brain ischemia induced in rat by middle cerebral artery occlusion. ACS Chem Neurosci 6(9):1517–1525. https://doi.org/10.1021/acschemneuro.5b00175

Proia P, Schiera G, Mineo M, Ingrassia AMR, Santoro G, Savettieri G, Liegro ID (2008) Astrocytes shed extracellular vesicles that contain fibroblast growth factor-2 and vascular endothelial growth factor. Int J Mol Med 21(1):63–67

Qiao H, Zhang R, Gao L, Guo Y, Wang J, Zhang R, Li X, Li C, Chen Y, Cao F (2016) Molecular imaging for comparison of different growth factors on bone marrow-derived mesenchymal stromal cells' survival and proliferation in vivo. Biomed Res Int 2016:1363902–1363910. https://doi.org/10.1155/2016/1363902

Rotschafer JH, Hu S, Little M, Erickson M, Low WC, Cheeran MC (2013) Modulation of neural stem/progenitor cell proliferation during experimental herpes simplex encephalitis is mediated by differential FGF-2 expression in the adult brain. Neurobiol Dis 58:144–155. https://doi.org/10.1016/j.nbd.2013.05.018

Seghezzi G, Patel S, Ren CJ, Gualandris A, Pintucci G, Robbins ES, Shapiro RL, Galloway AC, Rifkin DB, Mignatti P (1998) Fibroblast growth factor-2 (FGF-2) induces vascular endothelial growth factor (VEGF) expression in the endothelial cells of forming capillaries: an autocrine mechanism contributing to angiogenesis. J Cell Biol 141(7):1659–1673. https://doi.org/10.1083/jcb.141.7.1659

Shi YH, Bingle L, Gong LH, Wang YX, Corke KP, Fang WG (2007) Basic FGF augments hypoxia induced HIF-1-alpha expression and VEGF release in T47D breast cancer cells. Pathology 39:396–400. https://doi.org/10.1080/00313020701444549

Shi YH, Wang YX, Bingle L, Gong LH, Heng WJ, Li Y, Fang WG (2005) In vitro study of HIF-1 activation and VEGF release by bFGF in the T47D breast cancer cell line under normoxic conditions: involvement of PI-3K/Akt and MEK1/ERK pathways. J Pathol 205:530–536. https://doi.org/10.1002/path.1734

Shimizu F, Sano Y, Abe MA, Maeda T, Ohtsuki S, Terasaki T, Kanda T (2011) Peripheral nerve pericytes modify the blood-nerve barrier function and tight junctional molecules through the secretion of various soluble factors. J Cell Physiol 226(1):255–266. https://doi.org/10.1002/jcp.22337

Wang R, He W, Li Z, Chang W, Xin Y, Huang T (2014) Caveolin-1 functions as a key regulator of 17beta-estradiol-mediated autophagy and apoptosis in BT474 breast cancer cells. Int J Mol Med 34(3):822–827. https://doi.org/10.3892/ijmm.2014.1836

Xiang Y, Liu H, Yan T, Zhuang Z, Jin D, Peng Y (2014) Functional electrical stimulation-facilitated proliferation and regeneration of neural precursor cells in the brains of rats with cerebral infarction. Neural Regen Res 9(3):243–251. https://doi.org/10.4103/1673-5374.128215

Xu L, Wang L, Wen Z, Wu L, Jiang Y, Yang L, Xiao L, Xie Y, Ma M, Zhu W, Ye R, Liu X (2016) Caveolin-1 is a checkpoint regulator in hypoxia-induced astrocyte apoptosis via Ras/Raf/ERK pathway. Am J Physiol Cell Physiol 310(11):C903–C910. https://doi.org/10.1152/ajpcell.00309.2015

Xu Z, Han K, Chen J, Wang C, Dong Y, Yu M, Bai R, Huang C, Hou L (2017) Vascular endothelial growth factor is neuroprotective against ischemic brain injury by inhibiting scavenger receptor A expression on microglia. 142:700–709. https://doi.org/10.1111/jnc.14108

Yamashita T, Deguchi K, Sawamoto K, Okano H, Kamiya T, Abe K (2006) Neuroprotection and neurosupplementation in ischaemic brain. Biochem Soc Trans 34(6):1310–1312. https://doi.org/10.1042/BST0341310

Yang F, Liu Y, Tu J, Wan J, Zhang J, Wu B, Chen S, Zhou J, Mu Y, Wang L (2014) Activated astrocytes enhance the dopaminergic differentiation of stem cells and promote brain repair through bFGF. Nat Commun 5:5627. https://doi.org/10.1038/ncomms6627

Ye L, Yang Y, Zhang X, Cai P, Li R, Chen D, Wei X, Zhang X, Xu H, Xiao J, Li X, Lin L, Zhang H (2015) The role of bFGF in the excessive activation of astrocytes is related to the inhibition of TLR4/NFkappaB signals. Int J Mol Sci 17. https://doi.org/10.3390/ijms17010037

Ye LB, Yu XC, Xia QH, Yang Y, Chen DQ, Wu F, Wei XJ, Zhang X, Zheng BB, Fu XB, Xu HZ, Li XK, Xiao J, Zhang HY (2016) Regulation of caveolin-1 and junction proteins by bFGF contributes to the integrity of blood-spinal cord barrier and functional recovery. Neurotherapeutics 13(4):844–858. https://doi.org/10.1007/s13311-016-0437-3

Zhang Z, Chopp M (2002) Vascular endothelial growth factor and angiopoietins in focal cerebral ischemia. Trends Cardiovasc Med 12(2):62–66. https://doi.org/10.1016/S1050-1738(01)00149-9

Zhao Y, Pang Q, Liu M, Pan J, Xiang B, Huang T, Tu F, Liu C, Chen X (2017) Treadmill exercise promotes neurogenesis in ischemic rat brains via caveolin-1/VEGF signaling pathways. Neurochem Res 42(2):389–397. https://doi.org/10.1007/s11064-016-2081-z